International Journal of Multiphase Flow 35 (2009) 1001–1010

Contents lists available at ScienceDirect

International Journal of Multiphase Flow

journal homepage: www.elsevier.com/locate/ijmulflow

Prediction of the transition from stratified to slug flow or roll-waves in gas–liquid horizontal pipes

U. Kadri [a,*], R.F. Mudde [a], R.V.A. Oliemans [a], M. Bonizzi [b], P. Andreussi [b,c]

[a] Department of Multi-Scale Physics, Kramers Laboratorium, Delft University of Technology, Prins Bernhardlaan 6, 2628 BW Delft, The Netherlands
[b] TEA Sistemi SPA, Via Livinallono n.3, 20139 Milano, Italy
[c] University of Pisa, Pisa, Italy

ARTICLE INFO

Article history:
Received 3 April 2009
Received in revised form 7 July 2009
Accepted 7 July 2009
Available online 10 July 2009

Keywords:
Waves
Roll-waves
Slug flow
Gas–liquid pipe flow
Flow regime transition

ABSTRACT

In stratified gas–liquid horizontal pipe flow, growing long wavelength waves may reach the top of the pipe and form a slug flow, or evolve into roll-waves. At certain flow conditions, slugs may grow to become extremely long, e.g. 500 pipe diameter. The existence of long slugs may cause operational upsets and a reduction in the flow efficiency. Therefore, predicting the flow conditions at which the long slugs appear contributes to a better design and management of the flow to maximize the flow efficiency.

In this paper, we introduce a wave transition model from stratified flow to slug flow or roll-wave regimes. The model tracks the wave crest along the pipe. If the crest overtakes the downstream wave end before hitting the top of the pipe, a roll-wave is formed, otherwise a slug.

For model validation we performed measurements in air–water horizontal pipe flow facilities with internal diameters of 0.052 and 0.06 m. Furthermore, we made numerical calculations using a transient one-dimensional multiphase flow simulator (MAST) which adopts a four-field model. The model presented in this paper successfully predicts the evolution of waves and their transition into either slugs or roll-waves. It also predicts the formation time of slugs and roll-waves with a satisfactory agreement.

1. Introduction

The transportation of gas and liquid in horizontal pipes can lead to a number of flow patterns. A stratified flow pattern has the configuration of a continuous gas phase flowing on the top of the liquid phase. This pattern occurs at relatively low gas and liquid superficial velocities. At higher liquid superficial velocity waves may initiate at the interface. These waves can grow to reach the top of the pipe forming liquid plugs travelling in the pipeline, separated by large gas bubbles. This intermittent regime is characterized as slug flow. However, if the growth rate of the waves is insufficient it can be shown, from momentum and mass balances, that the crests of the growing waves move faster than the troughs (Lighthill et al., 1955). This behaviour might cause the crests to roll over the downstream end of the wave forming roll-waves.

1.1. Waves

The wave growth can be described by the Kelvin–Helmholtz instability as follows. The local gas velocity is highest in the neighbourhood of the wave crest so that the local gas pressure drops there. As a result, suction forces elevate the interface further toward the top of the pipe while gravity forces work at the opposite direction tending to stabilize the wave. At sufficient gas velocity the suction forces overcome gravity and the liquid level increases.

1.2. Transition to roll-waves

Jeffreys (1925) suggested theoretical relations to predict the initiation of roll-waves by using integral forms of momentum and mass balances and by examining the conditions under which a disturbance will grow. Hanratty and Hershman (1961) applied the theory proposed by Jeffreys (1925) to explain roll-wave transition and suggested initiation of roll-waves from predictions of conditions under which long wave disturbances occur in gas–liquid flows. They showed that their appearance is due to an instability in the flow. Soleimani and Hanratty (2003) claimed that the viscous long wavelength (VLW) theory (which is essentially the same as was used by Hanratty and Hershman (1961)) can be used to predict the initiation of roll-waves in a pipe flow. They concluded that as the gas superficial velocity increases the frequency of the roll-waves increases, and a larger critical superficial liquid velocity is required for the transition to slug flow.

1.3. Transition to slug flow

Taitel and Dukler (1976) suggested a critical condition for the gas velocity when gravity can no longer restore the fluctuating

* Corresponding author. Tel.: +31 27 83210; fax: +31 27 82838.
E-mail address: U.Kadri@tudelft.nl (U. Kadri).

0301-9322/$ - see front matter © 2009 Elsevier Ltd. All rights reserved.
doi:10.1016/j.ijmultiphaseflow.2009.07.002

pressure of the wave, taking into account non-linear effects using inviscid Kelvin–Helmholtz (IKH). The Taitel and Dukler approach is widely used to predict the transition to intermittent flow. This transition can be defined by one (or more) of three criteria: a viscous linear instability of a stratified flow to long wavelength disturbances; the stability of a slug; and a Kelvin–Helmholtz instability of a stratified flow.

The viscous linear stability analysis (viscous Kelvin–Helmholtz – VKH) done by Lin and Hanratty (1986) and Wu et al. (1987) describes waves on thin films over which air is blowing. They showed that the influence of the interfacial stress and the resisting stresses at the wall should be included. The theory of viscous long wavelength (VLW) predicts the transitions in gas–liquid systems at low gas velocities. It predicts the gas velocity for the appearance of long wavelength waves and their growth into a slug as reported by Woods and Hanratty (2000).

Hurlburt and Hanratty (2002) suggested that the transition to the slug region in a plot with superficial velocities of gas and liquid is predicted by the VLW model for low gas velocities, and by the slug stability model for high gas velocities. They argued that better predictions can be obtained if the interfacial friction factors are better estimated. The work of Andritsos and Hanratty (1987) together with other results Bontozoglu and Hanratty (1989) and Simmons and Hanratty (2001) provided a correlation for the interfacial friction factor for the air–water flows.

Woods and Hanratty (1999) suggested two main mechanisms for the transition to slug flow: (1) at low gas and liquid velocities, where the liquid flow rate is subcritical, large amplitude gravity waves may reach the top of the pipe forming a slug; whereas (2) at supercritical flow rates, slug formation is determined by coalescing roll-waves and can be described by a probabilistic process. Kadri et al. (2009) showed that the long slugs form only at low gas and liquid superficial velocities, i.e. via gravity waves.

In this paper, we consider the transition from stratified flow to slug flow or roll-wave regimes – slugs that may form by coalescing roll-waves are not addressed. In order to determine the evolution of waves we developed a simplified model that tracks the axial and vertical positions of the wave crest of a growing long wavelength wave in gas–liquid horizontal pipe flow. A linear assumption, for the momentum transfer from the gas phase to the wave crest, is made in order to calculate the axial velocity of the wave crest. The vertical displacement of the wave crest is calculated using an exponential wave growth based on a slug frequency correlation (Nydal, 1991). If the crest overtakes the downstream wave end before it reaches the top of the pipe, the crest rolls over the downstream wave end forming a roll-wave. Otherwise, at sufficiently high superficial velocities, if the wave crest bridges the pipe before approaching the downstream wave end, a slug is formed.

Constructing such a simplified theoretical model that successively approximates the transition from waves into slug flow or roll-waves has two major advantages: (I) the computing time of the current model is extremely low, and (II) physical parameters can be easily tracked within the different stages of the model.

For the validation of the model we performed wave growth time measurements using a high speed camera in a 137 m long air–water horizontal pipe flow of an internal diameter (i.d.) of 0.052 m. The measurements provide clearly the behaviour of the wave crest just before hitting the top of the pipe. Another set of experiments was carried out in a 16 m long air–water horizontal pipe flow of 0.06 m i.d. pipe at different gas and liquid superficial velocities. In this set of experiments we tracked the crest of growing waves and measured the slug/roll-wave formation time. The measurements were compared with the theoretical predictions of the current model at different gas and liquid superficial velocities. Moreover, theoretical predictions of different pipe sizes were tested against MAST, a transient one-dimensional multiphase flow simulator whose numerical framework is based on a multi-field approach as described by Bonizzi et al. (2009). MAST is capable to predict transitions from one flow pattern to another retaining the same set of closure laws and governing equations, provided that high spatial resolution of the computational grid is adopted.

A theoretical background including stability of stratified flow and slug stability model is presented in Section 2. The detailed analysis of the proposed model for the transition from stratified flow to slug flow or roll-wave regimes is given in Section 3. Section 4 provides an overview of the experimental setup and the methods used for performing the measurements. Details on the numerical tests by MAST are given in Section 5. Comparisons between theory and measurements, and theory and simulations are given in Section 6. Finally, the conclusions are presented in Section 7.

2. Theoretical background

2.1. A stratified flow pattern

A simplified geometric representation of the time-averaged stratified flow is considered prior to the transition to slug flow or roll-wave regimes. The pipe diameter is denoted by D. The length of the segments of the pipe circumference that are in contact with the gas and with the liquid are, respectively, S_G and S_L. The length of the gas–water interface is presented by S_i. The areas occupied by the gas and the liquid are denoted by A_G and A_L. The parameter h_L is the height of the liquid layer along the centerline. Given the pipe diameter, D, and any other parameter the remaining parameters are calculated using geometric considerations (e.g. Govier and Aziz, 1972).

Based on the simplified geometry, the momentum balances for the gas and liquid phases can be expressed by:

$$-A_G\left(\frac{dp}{dx}\right) - \tau_{WG}S_G - \tau_i S_i + \rho_G A_G g \sin\theta = 0; \quad (1)$$

$$-A_L\left(\frac{dp}{dx} - \rho_L g\cos\theta\frac{dh_L}{dx}\right) - \tau_{WL}S_L + \tau_i S_i + \rho_L A_L g \sin\theta = 0; \quad (2)$$

where ρ_G and ρ_L are the gas and liquid densities, θ is the inclination angle of the pipe from the horizontal. dp/dx is the pressure gradient, dh_L/dx is the liquid hydraulic gradient, g is the acceleration due to gravitational forces, τ_{WG} and τ_{WL} are the time-averaged resisting stresses of the gas and liquid phases at the wall, and τ_i is the resisting stress at the interface. The stresses τ_{WG}, τ_{WL} and τ_i are defined in terms of friction factors, which are calculated using the Blasius equation if $Re < 10^5$ and the wall roughness effect can be ignored, otherwise the Churchill equation is used (see Churchill, 1977). However, because of the presence of waves at the interface, the interfacial friction factor, f_i, becomes larger than the friction factor for a smooth surface, f_s. A number of previous works (Andritsos and Hanratty, 1987; Bontozoglu and Hanratty, 1989; Simmons and Hanratty, 2001; Hurlburt and Hanratty, 2002) suggest an estimation for interfacial friction factors (near the transition) for air–water flows from the following relations:

$$\frac{f_i}{f_s} = 2, \quad \text{smooth liquid surface} \qquad (U-u) \leqslant (U-u)_{\text{crit}}; \quad (3)$$

$$\frac{f_i}{f_s} = 5, \quad \text{wavy liquid surface} \qquad (U-u) \leqslant (U-u)_{\text{crit}}; \quad (4)$$

$$\frac{f_i}{f_s} = 5 + 15\left(\frac{h_L}{D}\right)^{0.5}\left[\frac{(U-u)}{(U-u)_{\text{crit}}} - 1\right], \qquad (U-u) > (U-u)_{\text{crit}}; \quad (5)$$

where U and u are the actual gas and liquid velocities, and $(U-u)_{\text{crit}}$ is the critical relative velocity at which waves become unstable.

Note that the flow is assumed to be varying slowly enough so that pseudo-steady-state assumptions can be made (e.g. $dh_L/dx = 0$ and

τ_{WG}, τ_{WL} and τ_i can be related to flow variables). Based on the pseudo-steady-state assumptions, Eqs. (1) and (2) are used to find the pressure gradient and the height of the liquid layer provided that the superficial velocities of the gas and the liquid are given.

2.2. Slug stability theory

Slug stability theory considers the rates of liquid adjoining or detaching from the slug at its front or back. The back of the slug is assumed to propagate together with the bubble at the bubble velocity C_B. The bubble velocity is modelled as a Benjamin bubble (Benjamin, 1968).

Slugs are defined *neutrally stable* (following Hurlburt and Hanratty, 2002) when the flow rate of liquid adjoining is equal to the rate at which liquid detaches ($Q_{in} = Q_{out}$). This also requires that the slug front and back velocities are equal, $C_F = C_B$. Applying the two conditions of neutral stability, and making a volumetric flow balance between the liquid entering the front and leaving the back result in a critical liquid area at the front of the slug below which it will be unstable (Hurlburt and Hanratty, 2002; Soleimani and Hanratty, 2003; Kadri et al., 2009):

$$\left(\frac{A_{L1}}{A}\right)_{\text{crit}} = \frac{(C_B - u_3)(1-\varepsilon)}{(C_B - u_1)}, \tag{6}$$

where ε is the void fraction in the slug, u_1 and A_{L1} are, respectively, the actual liquid velocity and liquid cross-sectional area downstream the slug, and u_3 is the actual liquid velocity in the slug. From Eq. (6) we calculate the minimum liquid height, $h_{L_{\min}}$, in front of a stable slug. A more detailed analysis of the slug stability theory can be found in Hurlburt and Hanratty (2002) and Soleimani and Hanratty (2003).

2.3. The liquid level downstream of the growing wave

The average liquid cross-sectional area of the stratified layer, $A_{L_{\text{avg}}}$, is calculated from the momentum balances for the stratified flow pattern, Eqs. (1) and (2). Following Kadri et al. (2009), substituting $A_L = A_{L_{\text{avg}}}$ and $A_G = A - A_{L_{\text{avg}}}$, Eq. (1) is written in the following form:

$$\left(\frac{dp}{dx}\right) = \frac{\tau_{WG}S_G + \tau_i S_i}{A - A_{L_{\text{avg}}}} - \rho_G g \sin\theta. \tag{7}$$

Plain stratified flow is reached when the pressure gradients of the two phases on the interface cancel. Therefore, substituting Eq. (7) in Eq. (2) and after basic algebra we obtain,

$$A_{L_{\text{avg}}} = A\frac{\tau_{WL}S_L - \tau_i S_i}{\tau_{WL}S_L + \tau_{WG}S_G}, \tag{8}$$

for a fully developed stratified flow.

In this paper, we do not consider the evolution of unstable slugs. Therefore, we only address problems that satisfy the following condition,

$$\left(\frac{A_{L_{\text{avg}}}}{A}\right) \geqslant \left(\frac{A_{L1}}{A}\right)_{\text{crit}}. \tag{9}$$

From Eq. (8) and geometric consideration we calculate the liquid height of the averaged stratified flow, $h_{L_{\text{avg}}}$.

3. A roll-wave/slug formation time model

In the model presented here, we address the formation of either slugs or roll-waves from growing waves. The waves are assumed to have a wavelength, λ, large compared to the average liquid height of the stratified flow, $h_{L_{\text{avg}}}$. Such waves have an average wave velocity, C, that depends on the liquid level alone,

$$C = \sqrt{g h_{L_{\text{avg}}}}. \tag{10}$$

The long wavelength waves grow in two different directions:

(1) *Growth in the vertical direction:* The local velocity of the gas phase above the rising wave crest increases. As a result, the pressure drops and local suction forces (associated with the Bernoulli effect) tend to elevate the surface in the neighbourhood of the wave crest, whereas gravity acts in the opposite direction tending to stabilize the wave surface. At sufficiently high gas velocities, the local suction forces overcome the gravitational forces and the liquid level surrounding the crest grows toward the top of the pipe.

(2) *Growth in the axial direction:* It can be shown, from the law of conservation of mass, that the wave crest propagates at a higher axial velocity than the wave trough (Lighthill et al., 1955). If the crest overtakes the downstream wave end, the crest will steepen and roll upon itself creating a roll-wave (Hanratty and Hershman, 1961).

In our model, we calculate the time required for the crest to reach the top of the pipe, t_y, and the time needed for the crest to approach the horizontal displacement of the downstream trough, t_x. If the crest reaches the top of the pipe before it approaches the downstream trough, the wave grows into a slug. On the other hand, if the crest approaches the downstream trough first, a roll-wave is generated. This is the outline of the model presented here:

$$\text{if} \quad t_y < t_x \quad \text{the wave evolves into a slug,} \tag{11}$$

$$\text{if} \quad t_x < t_y \quad \text{the wave evolves into a roll-wave.} \tag{12}$$

Note that, depending on the height of the liquid layer, a slug formed can either be a hydrodynamic slug with an average length of 30D or a long growing slug that may reach lengths that are 10 times greater.

3.1. The vertical growth time

We consider a long wavelength wave propagating over the average liquid height, $h_{L_{\text{avg}}}$, as given in Fig. 1 (top). In the figure, the term η_0 represents the initial amplitude of the wave. Following Kadri et al. (2007a,b), the growth rate of the amplitude is defined as

$$\frac{d\eta}{dt} = K\eta, \tag{13}$$

where t is the time, η is the amplitude of the wave, the parameter K is a non-linear growth defined as $K = C_1\mathbf{f}_S$ (Kadri et al., 2007b), and $\mathbf{f}_S$ is the slug frequency calculated with the correlation suggested by Nydal (1991):

$$\mathbf{f}_S = 0.088\frac{(U_{SL} + 1.5)^2}{gD}. \tag{14}$$

The definition of K based on the slug frequency is a logical choice, since the slug time ($1/\mathbf{f}_S$) is an actual limit for the average growth time of waves that evolve into slugs. The smaller the slug frequency is the greater the growth time becomes. The parameter C_1 is a constant that was chosen as $C_1 = 0.3$ for the best agreement with air–water horizontal pipe flow measurements (Kadri et al., 2007b). Solving Eq. (13) and substituting $K = 0.3\mathbf{f}_S$ results in,

$$\eta(t) = \eta_0 e^{0.3\mathbf{f}_S t}. \tag{15}$$

The initial amplitude, η_0, is estimated from the pressure fluctuations at the surface caused by turbulence (Phillips, 1957; Longuet-Higgins, 1952). Therefore, and to a first approximation, we consider the initial wave amplitude, η_0, to be proportional to the turbulence length scale, l_T. The proportionality between η_0 and l_T is expressed as function of D alone (see Appendix A). Thus, we

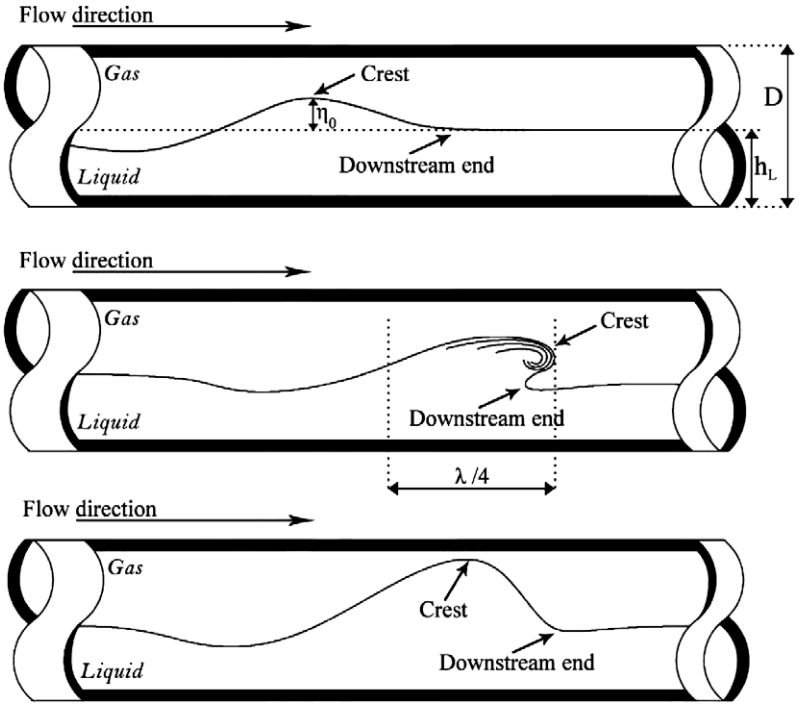

Fig. 1. Pictorial representation of a growing wave (top); the wave crest overtakes the downstream wave end forming a roll-wave (middle); the wave crest reaches the critical liquid height near the top of the pipe forming a slug (bottom).

write $\eta_0 = C_2 D$, where C_2 is the proportionality constant. A range of $0.01 < C_2 < 0.03$ is obtained, and for a maximum vertical growth time, the minimum value of the proportionality constant, $C_2 = 0.01$, is considered.

Using the amplitude growth rate (Eq. (15)), the time needed for the crest to hit the top of the pipe, t_y, is calculated. By substituting $t = t_y$ and $\eta(t = t_y) = D - h_{L_{avg}}$ in Eq. (15), we obtain the following relation for t_y:

$$t_y = \frac{1}{0.3\mathbf{f}_S} \ln \frac{D - h_{L_{avg}}}{\eta_0}. \tag{16}$$

3.2. The axial growth time

A roll-wave is formed when the crest overtakes the downstream wave end (see Fig. 1 (middle)). The distance between the crest and the downstream wave end is $\lambda/4$, as shown in the figure. The downstream end of the wave propagates with the wave at the propagation velocity C. Whereas due to the contribution of the momentum of the gas phase, the crest has an axial velocity:

$$U_{\text{crest}}(\eta) = \frac{\rho_G U + \rho_L C}{\rho_G + \rho_L}, \tag{17}$$

where U is the actual mean velocity of the gas phase at the crest, $U \equiv U_{SG}(A/A_G)$. Note that the cross-sectional area of the gas phase, A_G, at the crest decreases when the wave amplitude η grows, and therefore $U_{\text{crest}} = f(\eta)$.

The time needed for the crest to approach the downstream wave end can be determined from the relative velocity, and the distance between the crest and the downstream wave end,

$$t_x = \frac{\lambda/4}{U_{\text{crest}}(\eta) - C}. \tag{18}$$

Following Kadri et al. (2009), the term λ is calculated from the wave velocity ($\lambda = C/\mathbf{f}_w$) and the relation $\mathbf{f}_w = c_w \mathbf{f}_S$ by Tronconi (1990) for the slug and the wave frequencies, $\mathbf{f}_S$ and $\mathbf{f}_w$, as follows:

$$\lambda = \frac{C}{c_w \mathbf{f}_S}, \tag{19}$$

where c_w is a constant equal to 2 for air–water systems (Tronconi, 1990). Note that Woods and Hanratty (1999) reported slug frequency measurements to be inconsistent with the relation between slug frequency and wave frequency by Tronconi (1990) (e.g. Eq. (19)). However, here we use Eq. (19) only to estimate a realistic value of λ, which plays no role for predicting the vertical growth time (16).

4. Experiments

Experiments have been carried out in two multiphase flow laboratory facilities. The first facility, located at the *Kramers Laboratorium of Fysische Technologie* (KLFT) at TU Delft, The Netherlands, is denoted as the KLFT flow loop. In this facility, we investigated the behaviour of wave crests of growing waves just before they evolve into slugs. The second facility is the NTNU (Norwegian University of Science and Technology) flow loop located in Trondheim, Norway. Here, we tracked growing waves using a moving camera, and measured the time needed for initial disturbances to evolve into either roll-waves or slugs. Descriptions of the experimental setup of each facility are given in the following sub-sections.

4.1. The KLFT flow loop

The flow loop used in the experiments consists of a 137 m long horizontal pipeline with a 0.052 m i.d. pipe. The pipe is made of Perspex (plexiglas) to allow visual observations of the flow conditions. The experiments are performed at atmospheric pressure with gas and liquid being air and water, respectively. The two phases are combined at the inlet in a Y-shaped section. The gas enters from the top in a horizontal direction, in order to prevent the impact of gas-jet coming from above. At the outlet, the last element of the pipe is connected to a short near-horizontal hose.

The hose enters a larger diameter pipe through which the liquid returns down to the storage tank positioned 5 m below, and the gas is allowed to escape. A sketch of the experimental setup is given in Fig. 2. In the sketch L_{pipe} stands for the length of the pipeline test section.

The shape and movement of the growing waves are measured by means of a high speed camera (Olympus, i-SPEED). The camera is positioned at 4 locations along the pipe at: 2–3.5, 4, 7.5, and 13 m from the inlet (see Fig. 2). The locations are denoted by 1, 2, 3 and 4, respectively. The camera is setup such that the field of view in one image covers a length of 0.5 m, while still having high enough resolution to resolve the gas–liquid interface accurately. The frame rate of the camera is 955.5 frames per second (fps), with an uncertainty of 2 fps. Images of the growing waves were evaluated by tracking their position in time. At location 1, we tracked the crest of growing waves just before they hit the top of the pipe creating slugs. For that matter, the camera at position 1 had to be located between 2 and 3.5 m from the inlet depending on the gas and liquid superficial velocities. At the other three locations we tracked the downstream front and back of the slugs formed to ensure that the behaviour of the liquid downstream and upstream the slugs is similar in all measurements. The experiments were performed at constant gas and liquid superficial velocities being 1.5—3 and 0.2—0.4 m/s, respectively. Fig. 3 presents three images by the camera capturing the propagation of a growing wave (see top picture), the "jump" of the crest reaching the top of the pipe (middle picture), and the propagation of the formed slug (bottom picture). It is noticeable that the exit geometry and the fact that the measurements were performed at the initial part of the pipe ensure independence of the liquid holdup from any outlet effect.

The aim of this set of measurements is to show the development of the growing waves, especially during the "jump". Although the model presented in this paper does not consider this "jump", we show that the difference between the slug growth time calculations using the model and the measurements is negligible. Hence, the slug growth time can be approximated by calculating the time needed for the crest to reach the top of the pipe.

4.2. The NTNU flow loop

The experiments in the NTNU flow loop were done for a two phase air–water horizontal pipe flow. The test loop is 16 m long with a 0.06 m i.d. pipe. The pipe is made of straight transparent plexiglass and configured as an open loop system so that the pressure at the outlet is atmospheric. The two phases are combined at the inlet in a Y-shaped section, where the gas enters at 45° from the top and the liquid is introduced axially. At the outlet, the liquid is allowed to drop downwards. A sketch of the experimental setup is given in Fig. 4.

Two different measurement techniques were installed. The first consists of 4 ring probes located along the pipe at: 3.39, 5.91, 10.77, and 13.13 m from the inlet. The probes were used to record the time dependent liquid height behaviour. The probes were primarily used as slug detectors. In the second measurement technique the growing waves were tracked using a moving camera (webcam) (see Fig. 4). The camera slides over a track along the pipeline at a speed that is manually controlled. The time that takes the waves to evolve into either slugs or roll-waves was measured.

Two sets of experiments were performed, each at different constant superficial liquid velocities, 0.17 and 0.22 m/s, and varying superficial gas velocities, 0.5—6 m/s. For consistency, the following procedure was applied to all measurements: (a) the superficial gas and liquid velocities are set to the desired values – the liquid valve was 50% opened for $U_{SL} = 0.17$ m/s and 75% for $U_{SL} = 0.22$ m/s, and the liquid pump frequency was 30–35 Hz; (b) the pump frequency is reduced to 10 Hz for 10 s – this was necessary in order to reduce the liquid level close to $h_{L_{avg}}$, and to have a smoother interface; (c) the pump is set back to the original value and the time measurement starts; and (d) each time measurement is stopped when the crest of a growing wave rolls over the downstream wave end or hits the top of the pipe. The stopping criterion is based on visual observations and verified using the time dependent liquid height measurements. Note that only the first slug or roll-wave were considered in each measurement. Therefore, the exit effects of slugs or roll-waves are irrelevant. It is also worth noting that perturbations that may appear at the interface due to procedures (b) and (c) result in shorter growth times in the measurements. However, the appearance time of perturbations on a "perfectly" smooth interface is associated with a turbulence time scale in gas and liquid, that is much shorter than the wave growth time. Therefore, the effect of induced perturbations on the total measuring time is negligible.

5. Numerical tests

The numerical code used to conduct computational tests is MAST (Multiphase Analysis and Simulation of Transitions). The simulator, in the case of gas–liquid flows, solves the governing equations of the flow (mass, momentum and pressure) for each field which locally maybe generated inside each control volume (liquid continuous, liquid dispersed – droplets, gas continuous,

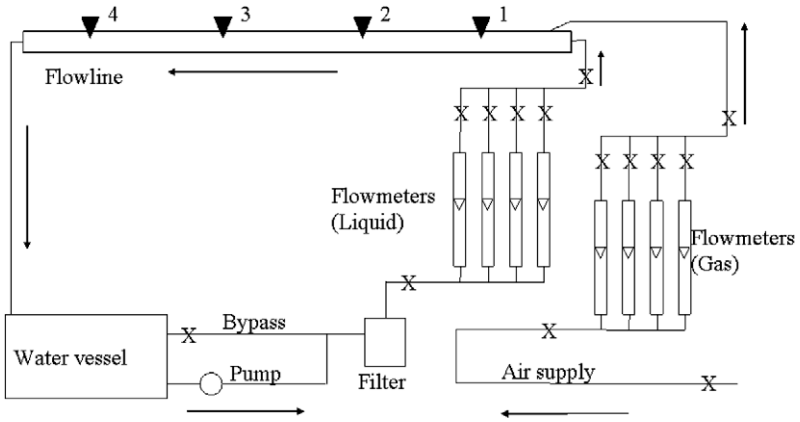

Fig. 2. Sketch of the KLFT experimental setup. Air–water horizontal pipe flow, $L_{pipe} = 137$ m, $D = 0.052$ m. The valves are indicated by ×. The 4 positions of the camera are indicated by (▼). Distance from the inlet: (1) 2—3.5 m; (2)4 m; (3)7.5 m; and (4)13 m.

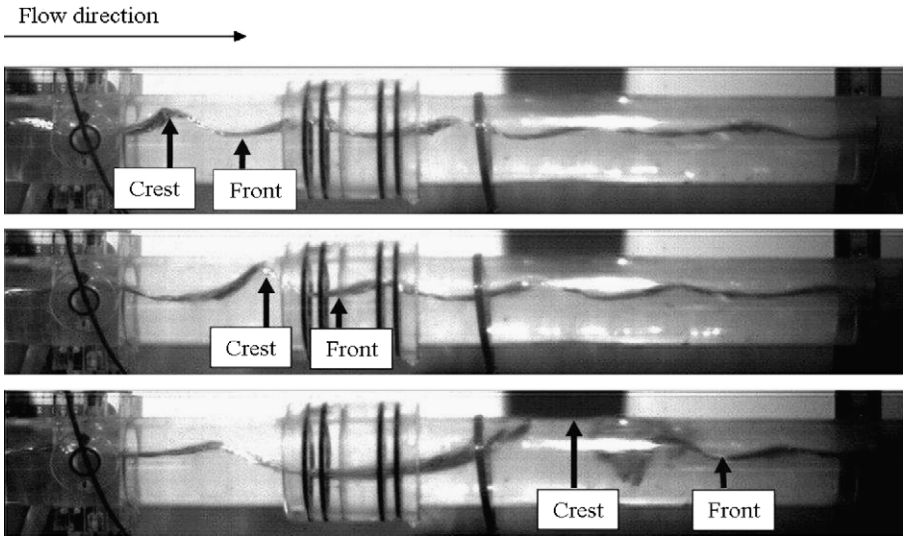

Fig. 3. Three images captured by the camera. Top: the propagation of a growing wave. Middle: the "jump" of the crest reaching the top of the pipe. Bottom: slightly after the slug is formed.

gas dispersed – bubbles). In this approach, mass conservation is enforced.

The governing equations of the flow are discretised on a staggered grid arrangement using a fully explicit discretisation in time and a first order upwind scheme for the spatial terms. The developed methodology allows the prediction of the flow pattern which prevails in each computational node retaining the same set of closure laws and governing equations. Hence, different fields may exist from control volume to control volume, depending on the flow pattern which prevails. Qualitatively we identify the local flow pattern that prevails in each computational cell as follows:

(1) *Stratified flow:* Stratified layers (of continuous gas and continuous liquid with possibly some entrained gas–dispersed gas field) with low void fraction fluctuations (no distinction is made between wavy and smooth regimes).
(2) *Annular flow:* Stratified layers (a layer of continuous gas with dispersed liquid and a layer of continuous liquid) where the liquid layer tends to wet the whole perimeter of the pipe wall and the gas flows in the core.
(3) *Slug flow:* Stratified layers with large void fraction fluctuations which do bridge the pipe, causing regions with very thin stratified gas layers (i.e. the liquid film is dominated by the presence of two stratified layers – continuous gas with possibly dispersed liquid, and continuous liquid with in general dispersed bubbles; the slug body is dominated by a continuous liquid film with dispersed gas with a very thin continuous gas layer on top).
(4) *Bubbly flow:* The pipe is fully bridged with no regions where there are stratified gas layers that are not very thin (continuous liquid with dispersed gas bubbles).

Unstable waves may grow until the pipe is fully bridged and a slug is generated. Slugging is predicted because the governing equations are capable to capture the viscous Kelvin–Helmholtz instabilities that lead to flow pattern transition from stratified to slug flow (Issa and Kempf, 2003). In order to ensure that these instabilities are not smeared out by numerical diffusion, a fine numerical mesh is adopted with a spatial resolution of some pipe diameters. The growth of the instabilities is then an outcome of

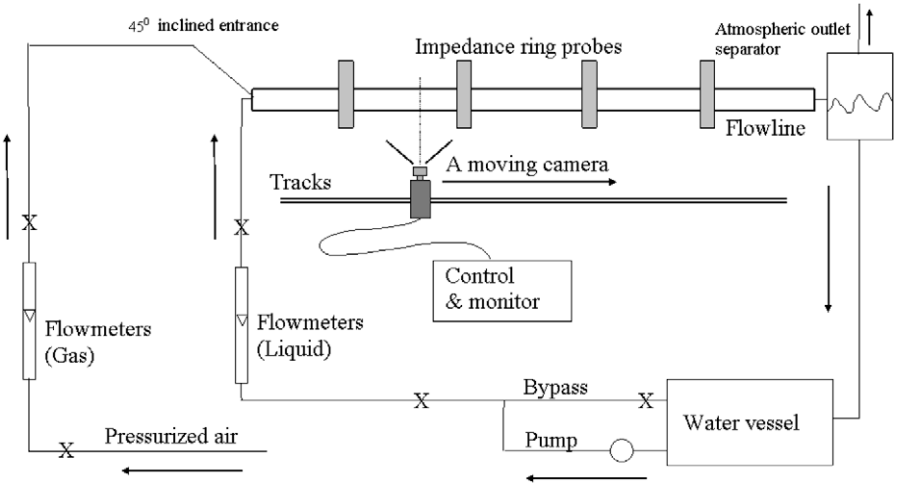

Fig. 4. Sketch of the NTNU experimental setup, the position of the impedance ring probes, and the moving camera track. Air–water horizontal pipe flow, $L_{pipe} = 16$ m, $D = 0.06$ m. The valves are indicated by $\times$.

the transient numerical solution of the equations. When slugging occurs, regardless of its specific nature (hydrodynamic, terrain-induced or severe), trains of slugs are generated automatically. Provided that reasonable closure laws (i.e. friction factors) are adopted, MAST has the capability to predict the correct flow pattern that results from the boundary and geometry conditions under investigation.

Fig. 5 shows typical profiles of the liquid holdup and gas velocity at different time instants for a wave which grows and eventually leads to hydrodynamic slugging for gas–liquid horizontal pipe flow. The pipe is 137 m long with 0.052 m i.d. (the KLFT facility), the gas and liquid phases are air and water travelling at $U_{SG} = 8$ and $U_{SL} = 0.3$ m/s, respectively.

Slugs of different sizes may be generated, depending on the pipe geometry and flow conditions, leading to a slug length distribution. The simulator, MAST, gives estimates of the average slug length as shown in Fig. 5 of the paper by Bonizzi et al. (2009), where predictions by MAST are compared with the measurements of Nydal et al. (1992) for air–water flow in a horizontal 0.05 *m* i.d. pipe at $U_{SL} = 0.6$ and 2.4 m/s.

The robustness of the slug criterion can be appreciated by referring to Fig. 7 of the paper by Bonizzi et al. (2009), where predictions of the critical height of the liquid layer at the transition to slug flow for air–water horizontal pipe flow at atmospheric pressure are plotted against U_{SG} and compared with measurements by Andritsos et al. (1989) and the theoretical transition boundary according to Hurlburt and Hanratty (2002). The accuracy of the criteria used for identification, noting that the closure relationships are not adjusted, is satisfactory. For the tests presented in this paper, the closures proposed by Taitel and Dukler (1976) were selected.

6. Results

In this section, we compare theoretical calculations, of the wave growth and the formation time of slugs and roll-waves, with measurements and simulations. A summary of the properties of the different systems is found in Table 1. For all calculations presented in this paper the lowest initial wave amplitude was applied in order to obtain the largest growth time of the wave crest, hence $C_2 = 0.01$ is chosen (see Appendix A).

6.1. Crest growth near the pipe top

Measurements of growing waves just before they hit the pipe top for air–water horizontal flow are presented in Fig. 6. The measurements were carried out in a 137 m long pipe with 0.052 m i.d. at the KLFT flow loop. A description of the experimental setup is found in Section 4.1. The subplots in Fig. 6 show the liquid holdup at the crest, $(h_L/D)_{\text{crest}}$, as function of time, t, at $U_{SG} = 1.85$ m/s and different superficial liquid velocities. The average liquid holdup is denoted by $(\times)$, whereas the minimum and maximum values of the holdup are represented by the error-bars. The solid line represent theoretical predictions of the crest growth from η_0. The wave grows exponentially until the top of the pipe is reached. A zoom over the measurement region is given on the right hand side of each subplot.

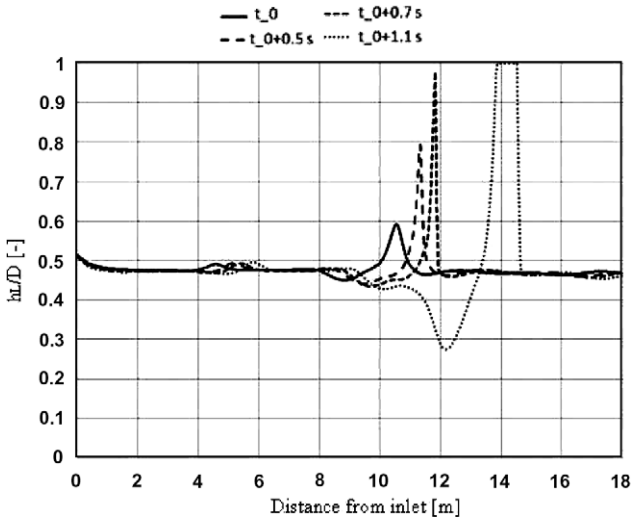

Fig. 5. Hydrodynamic instabilities in the KLFT loop calculated by MAST, for air–water 0.052 m i.d. pipe, $U_{SG} = 8$ and $U_{SL} = 0.3$ m/s.

In the subplots (a), (b) and (c) we see that the time needed for a growing crest before the "jump" is two orders of magnitude greater than the time needed for the crest to hit the top of the pipe (during the "jump"). This observation is true for all superficial velocities of gas and liquid in subplots (a), (b) and (c) of Fig. 6.

The measurements in subplots (a), (b) and (c) (in the zoom area) are for $U_{SG} = 1.85$ and $U_{SL} = 0.2, 0.3$ and 0.4 m/s, respectively. Here we see that increasing the superficial liquid velocity (at fixed U_{SG}) results in a shorter "jump time" being: 0.09, 0.06 and 0.04 s for subplots (a), (b) and (c), respectively. The "jump time" in subplot (b) is about two times slower than in subplot (c), and slightly faster than the "jump time" in subplot (a). A possible reason for this behaviour is the following. The stratified (initial) liquid height is larger for larger U_{SL} (Eq. (8)), and the actual gas velocity at the crest is constant for fixed U_{SG}. However, the total mass of liquid above the stratified liquid level is smaller for larger U_{SL} (and so is the potential energy). Therefore, the suction forces (e.g. Bernoulli effect) acting on the crest will result in a higher growth rate of the crest for larger U_{SL}.

In the case of subplot (b), the wave crest moves with an average velocity $U_{\text{crest}} = 0.7$ m/s, and the "jump" occurs after approximately 17 s. Thus, the wave crest moves a distance of 12 m, from the inlet, just before the slug is formed. This formation distance is well predicted by MAST, as shown by the dashed line $(t_0 + 0.7\text{ s})$ in Fig. 5.

6.2. Prediction of roll-wave/slug formation time

Theoretical calculations of the time needed for the wave crest to evolve into a roll-wave or a slug (t_x and t_y, respectively) are compared with measurements and numerical calculations by MAST in Fig. 7. The measurements were carried out in a 16 m pipe with a 0.06 m i.d. at NTNU. A description of the experimental setup and the numerical calculations are found in Sections 4.2 and 5, respectively. Fig. 7 presents the time needed for a growing wave to form either a slug or a roll-wave as a function of the superficial gas velocity, U_{SG}. In the figure, the superficial liquid velocity $U_{SL} = U_{SL_{\min}}$, where $U_{SL_{\min}}$ is the minimum velocity required for the transition to slug flow. $U_{SL_{\min}}$ is calculated iteratively from the gas and liquid momentum balances (Eqs. (1) and (2)) for the liquid height $h_{L_{\min}}$. The stars $(*)$ represent slug measurements, the plus signs $(+)$ are roll-wave observations, the bullets $(\bullet)$ and the circles $(\circ)$ are simulations by MAST for slugs and roll-waves, respectively.

Table 1
Summary of system properties.

	Air–water system
Pipe diameter [m]	0.025, 0.052, 0.06, 0.095
Pressure [Pa]	1×10^5, 2×10^5
Interfacial tension [N/m]	0.07
Gas density [kg/m^3]	1.2
Gas viscosity [kg/ms]	1.8×10^{-5}
Liquid density [kg/m^3]	1000
Liquid viscosity [kg/ms]	0.001

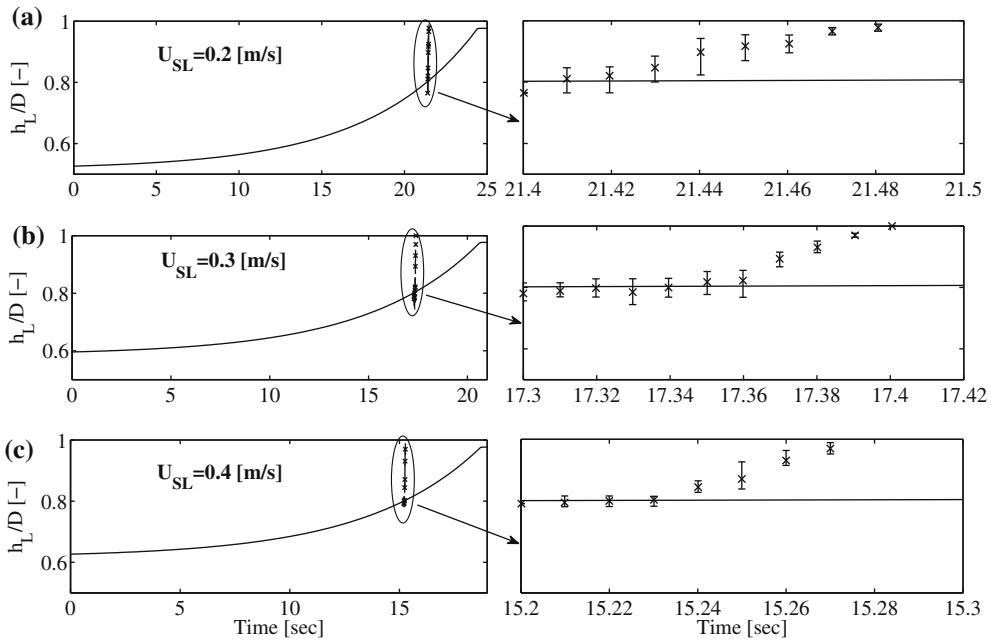

Fig. 6. Prediction of the wave crest growth, and time measurements (×) of the crest during the "jump", just before a slug is formed, for air–water flow in a horizontal $D = 0.052$ m pipe and $U_{SG} = 1.85$ m/s.

The dashed lines (--) are theoretical calculations of t_x (Eq. (18)), and the solid lines (-) represent theoretical calculations of t_y (Eq. (16)). The arrows indicate the curves for which either t_x or t_y is shortest, indicating a transition boundary from stratified to slug or roll-waves, respectively.

In Fig. 7 the model predicts that the slug/roll-wave formation time increases and then decreases with U_{SG}, and the intersection point between (t_x and t_y) successfully predicts the transition from growing regular gravity waves to roll-waves. Note that slugs may still form in the roll-wave region by coalescence between roll-waves or if the superficial liquid velocity is further increased. Increasing the superficial liquid velocity results in shorter transition times from stratified wavy to slug flow. This is clearly observed at low U_{SG}, which is not surprising since introducing larger U_{SL} results in a larger initial liquid height. Therefore, the distance between the wave crest and the top of the pipe becomes shorter. At sufficient liquid height, the wave crest will be unable to approach the downstream wave end before hitting the top of the pipe. Thus, a slug is formed.

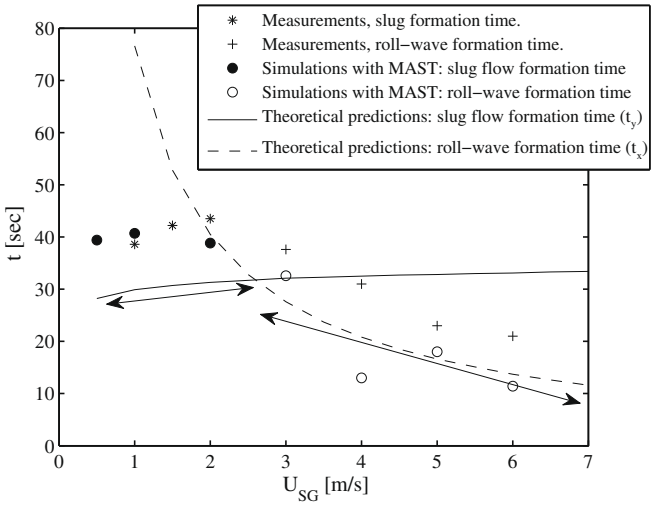

Fig. 7. Theoretical predictions of t_y and t_x, compared with slug and roll-wave measurements for air–water horizontal pipe flow at $U_{SL} = U_{SL_{min}}$ and $D = 0.06$ m.

6.3. Formation time predictions for different pipe diameters

We have performed simulations with MAST for horizontal air–water flow in pipes with diameters of 0.025, 0.052, and 0.095 m. The aim of the simulations is to investigate the diameter scaling of the transitions from stratified to slug and roll-wave regimes, where no experimental data is available for the flow regime transitions considered. Figs. 8–10 compare theoretical predictions of t_y and t_x with the simulations. The simulations for the slug flow and roll-wave cases are denoted by (■) and (□), respectively. The solid (-) and the dashed lines (--) represent theoretical calculations of t_x and t_y, respectively. The simulations and the model predictions have been performed at $U_{SL} = U_{SL_{min}}$. Note that increasing the pipe size requires larger $U_{SL_{min}}$ for the transition from stratified to slug flow.

In Fig. 8 the calculations were done for a 0.025 m i.d. pipe. At low U_{SG}, the time needed for the wave to hit the top of the pipe (t_y) grows with U_{SG}. A possible reason for that is the lower initial liquid height of the stratified flow due to the increase of the superficial gas velocity (Eq. (8)). The lower the initial height is, the larger the (vertical) distance needed to be travelled by the wave crest in order to hit the top of the pipe, and thus t_y increases. At large U_{SG}, and if U_{SL} is low enough, roll-waves are formed. Their formation is related to the relative velocity between the crest and the downstream wave end as given by Eq. (17). By increasing U_{SG}, the crest moves faster toward the downstream wave end resulting in shorter time for the formation of roll-waves.

For a larger pipe $D = 0.052$ m, presented in Fig. 9, we notice that the time needed for the wave to reach the top of the pipe increases. This can be explained by the larger vertical distance to be travelled by the wave crest due to the larger pipe diameter. The same behaviour is found for the pipes with diameters of 0.06 and 0.095 m presented in Figs. 7 and 10.

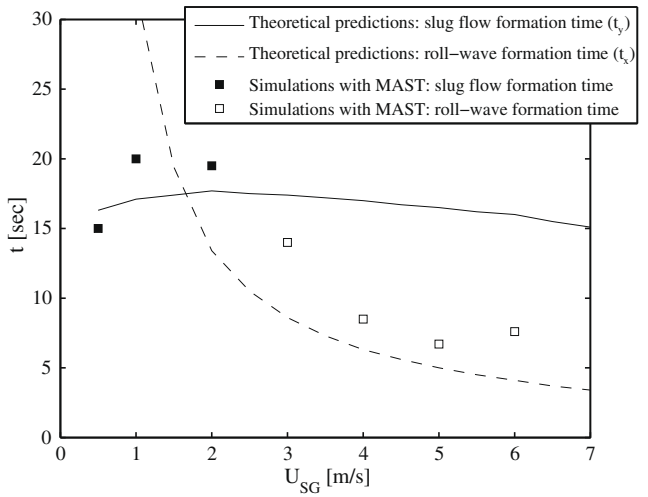

Fig. 8. Simulations and theoretical predictions of t_y and t_x for air–water horizontal pipe flow at $U_{SL} = U_{SL_{min}}$ and $D = 0.025$ m.

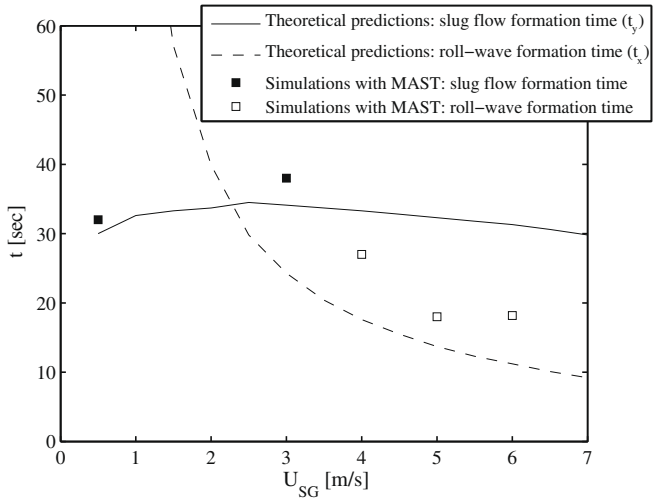

Fig. 9. Simulations and theoretical predictions of t_y and t_x for air–water horizontal pipe flow at $U_{SL} = U_{SL_{min}}$ and $D = 0.052$ m.

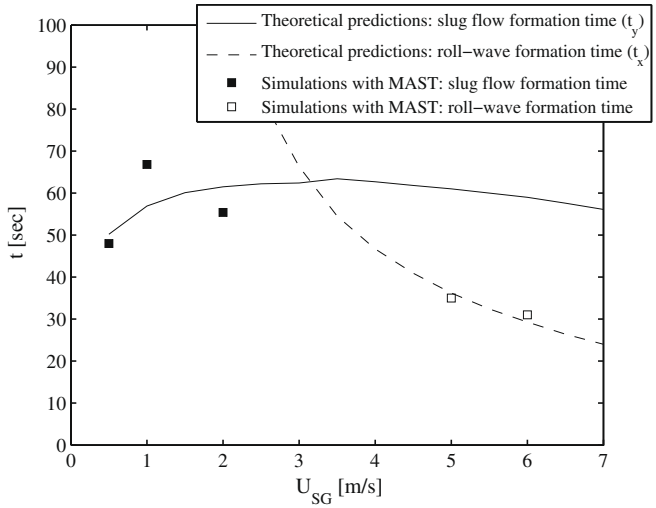

Fig. 10. Simulations and theoretical predictions of t_y and t_x for air–water horizontal pipe flow at $U_{SL} = U_{SL_{min}}$ and $D = 0.095$ m.

6.4. Critical Froude number for the transition

A significant result of the model is the relation between the pipe size and the transition from regular gravity waves (forming slug flow) to roll-wave regions. Defining $U_{SG_{crit}}$ as the critical superficial gas velocity where $t_y = t_x$, we find that $U_{SG_{crit}}$ increases with pipe size. In Figs. 8, 9, 7 and 10, $U_{SG_{crit}} \simeq 2.3, 3.4, 3.6$ and 4.1 m/s, respectively. Defining a Froude number $Fr_{crit} = \sqrt{\rho_G U^2_{SG_{crit}}/(\Delta\rho g D)}$, where $\Delta\rho = \rho_L - \rho_G$, we obtain that $Fr_{crit} \simeq 0.15$ is the critical Froude number at which the transition from slug flow (formed by gravity waves) to roll-waves occurs, for the different pipe diameters and $U_{SL_{min}}$ in Figs. 8, 9, 7 and 10.

This result agrees well with previous work by Woods and Hanratty (1999) who showed that the flow becomes supercritical, at $U_{SG} > 4$ m/s (that is at $Fr_{crit} > 0.16$), and slug formation is determined by coalescing roll-waves, whereas at lower U_{SG} slugging is reached when large wavelength waves reach the top of the pipe. They also noted that the minimum U_{SG} required for the transition from stratified to slug flow increases with the pipe size, which agrees with the behaviour of $U_{SG_{crit}}$ for the transition from slug flow to roll-wave region, as aforementioned.

7. Conclusions

(1) The evolution of long wavelength waves in horizontal pipes may result in different flow patterns in the pipe. If the wave crest reaches the top of the pipe a slug may form. However, if the crest overtakes the downstream wave end (before it reaches the top of the pipe) a roll-wave is formed.

(2) A "jump" in the liquid phase toward the top of the pipe is observed just before the wave crest bridges the pipe. A possible reason for this "jump" is the suction forces acting in the neighbourhood of the crest. The suction forces may become large enough to elevate the liquid surface as the actual gas velocity becomes relatively high due to the exponential decrease of the gas cross-sectional area at the crest.

(3) Measurements carried out in a 137 m long horizontal pipeline with a 0.052 m i.d. show that the time required for a wave to reach the height at which the crest "jumps" toward the top of the pipe, is much longer than the "jump time". Increasing the superficial liquid velocity results in shorter "jump" time.

(4) A wave transition model was presented. The model is based on calculating the time required for a long wavelength wave with a small initial amplitude, on the order of the turbulent length scale, to grow and reach the top of the pipe (see Eq. (16)), and the time it takes the axial propagation of the wave crest to overtake the downstream wave end (see Eq. (18)). The model predicts the transition from stratified flow to slug flow or roll-wave regimes for different pipe diameters and different gas and liquid superficial velocities.

(5) The model predicts a number of important observations regarding the behaviour of slug/roll-wave formation time: (a) increasing the superficial liquid velocity results in shorter transition times from stratified wavy to slug flow; (b) at relatively low U_{SG}, the formation of slug/roll-wave time increases with increasing U_{SG}, which is a result of the lower initial stratified height; however, (c) at relatively high U_{SG}, due to the domination of inertial forces, the formation time decreases with increasing U_{SG} and a roll-wave is formed; and (d) increasing the pipe size results in larger axial growth compared to the growth of the vertical direction, making the appearance of long slugs less likely.

(6) Numerical simulations have been carried out using a transient one-dimensional multiphase flow simulator in order to investigate the diameter scaling of the transitions from stratified to slug and roll-wave regimes. Comparing predictions by the model with the simulations we found that increasing the pipe diameter results in larger formation times for both t_y and t_x. However, since t_x is a function of both vertical and axial displacements of the crest, its sensitivity to a change in the pipe diameter is greater. As a result, larger U_{SG} is required for the transition from slug flow (formed by regular gravity waves) to roll-wave regimes.

(7) Based on predictions by the model presented in this paper we obtained a critical densimetric gas Froude number, $Fr \simeq 0.15$, for the transition from regular growing gravity waves, to roll-wave regimes. The critical Froude number was obtained for superficial velocities close to the transition to slug flow.

(8) The accuracy of the modelling could be improved if the interfacial friction factor at transition, the wave length, and the gas entrainment were better known over a wider range of flow conditions. The theories applied in the modelling are sensitive to the value of the interfacial friction factor which is of a critical importance at all flow rates. Whereas, the accuracy in the wave length and the gas entrainment (which was neglected in this paper) becomes important at relatively large flow rates.

Acknowledgements

The authors wish to thank Prof. O.J. Nydal for his hospitality at NTNU which made the measurements possible. This research is part of the research project: "Long liquid slugs in stratified gas/liquid flow in horizontal and slightly inclined tubes", sponsored by STW (Dutch Foundation for Technological Research).

Appendix A

The initial wave amplitude, η_0, is assumed to be half the turbulence length scale, l_T, in a fully developed pipe flow:

$$\eta_0 = \frac{l_T}{2}, \tag{20}$$

where

$$l_T = 0.07 D_{HG}. \tag{21}$$

The parameter D_{HG} is the hydraulic diameter of the gas phase give by

$$D_{HG} = \frac{4A_G}{S_i + S_G}. \tag{22}$$

From Eq. 8, we calculate the range of the normalized average gas area for the superficial gas and liquid velocities and pipe diameters considered in this paper as follows:

$$0.2 \lesssim \frac{A_{G_{avg}}}{D^2} \lesssim 0.7. \tag{23}$$

Using geometric relations to calculate S_i and S_G (e.g. Govier and Aziz, 1972) we obtain:

$$2 \lesssim \frac{S_i + S_G}{D} \lesssim 3. \tag{24}$$

Substituting Eqs. (23) and (24) into Eq. (22) results in a lower and upper values of D_{HG} as function of the pipe diameter:

$$0.4D \lesssim D_{HG} \lesssim 0.9. \tag{25}$$

Substituting Eqs. (25), (24), (23), (22) and (21) into Eq. (20) we obtain the following range for the initial amplitude:

$$0.01D \lesssim \eta_0 \lesssim 0.03D. \tag{26}$$

In order to obtain the maximum growth time of the crest we consider the smallest possible initial wave amplitude, $\eta_0 = 0.01D$. Hence, the constant $C_2 = 0.01$. It is noticeable that when operating at larger pressure the lower value of D_{HG} increases, due to momentum considerations. As a result C_2 should be modified ($C_2 > 0.01$). However, C_2 cannot be larger than 0.03 since the upper value of D_{HG} decreases with the pressure, due to the increase in the minimum liquid height downstream that is required for the formation of slugs (Eq. (6)). As a result, the upper value of C_2 decreases with the pressure (thus $0.01D < C_2 < 0.03D$).

References

Andritsos, N., Hanratty, T.J., 1987. Influence of interfacial waves in stratified gas–liquid flows. AIChE J. 33, 444–454.
Andritsos, N., Williams, L., Hanratty, T.J., 1989. Effect of liquid viscosity on the stratified–slug transition in horizontal pipe flow. Int. J. Multiphase Flow 15, 877–892.
Benjamin, T.B., 1968. Gravity currents and related phenomena. J. Fluid Mech. 31, 209–248.
Bonizzi, M., Andreussi, P., Banerjee, S., 2009. Flow regime independent, high resolution multi-field modelling of near-horizontal gas–liquid flows in pipelines. Int. J. Multiphase Flow 35, 34–46.
Bontozoglu, V., Hanratty, T.J., 1989. Wave height estimation in stratified gas–liquid flows. AIChE J. 35, 1346–1350.
Churchill, S.W., 1977. Friction-factor equation spans all fluid-flow regimes. Chem. Eng. 7, 91.
Govier, G.W., Aziz, K., 1972. The Flow of Complex Mixtures in Pipes. Van Nostrand Reinhold Co., NY. p. 563.
Hanratty, T.J., Hershman, A., 1961. Initiation of roll waves. AIChE J. 7, 488–497.
Hurlburt, E.T., Hanratty, T.J., 2002. Prediction of the transition from stratified to slug and plug flow for long pipes. Int. J. Multiphase Flow 28, 707–729.
Issa, R.I., Kempf, M.H.W., 2003. Simulation of slug flow in horizontal and nearly horizontal pipes with the two-fluid model. Int. J. Multiphase Flow 29, 69–95.
Jeffreys, H., 1925. The flow of water in an inclined channel of rectangular section. Phil. Mag. 49, 793–807.
Kadri, U., Mudde, R.F., Oliemans, R.V.A., 2007a. On the prediction of the transition from stratified flow to roll waves and slug flow in horizontal pipes. In: Proceedings 13th International Conference on Multiphase Production Technology, vol. 13, Edinburgh, Scotland, pp. 65–78.
Kadri, U., Mudde, R.F., Oliemans, R.V.A., 2007b. On the development of waves into roll waves and slugs in gas–liquid horizontal pipe flow. In: Proceedings 6th International Conference on Multiphase Flow, vol. 6, Leipzig, Germany, pp. 332.
Kadri, U., Zoeteweij, M.L., Mudde, R.F., Oliemans, R.V.A., 2009. A growth model for dynamic slugs in gas–liquid horizontal pipes. Int. J. Multiphase Flow 35, 439–449.
Lighthill, M., Whitman, G., 1955. On kinematics of waves: part 1 and 2. Proc. R. Soc. Lond. A229, 281–345.
Lin, P.Y., Hanratty, T.J., 1986. Prediction of the initiation of slugs with linear stability theory. Int. J. Multiphase Flow 12, 79–98.
Longuet-Higgins, M.S., 1952. On statistical distribution of the heights of sea waves. J. Mar. Res. 11, 245–266.
Nydal, O.J., 1991. An experimental investigation of slug flow. Ph.D. Thesis, University of Oslo, Department of Mathematics, Oslo, Norway.
Nydal, O.J., Pintus, S., Andreussi, P., 1992. Statistical characterization of slug flow in horizontal pipes. Int. J. Multiphase Flow 18, 439–453.
Phillips, O., 1957. On the generation of waves by turbulent wind. J. Fluid Mech. 2, 417–445.
Simmons, M.J.H., Hanratty, T.J., 2001. Transition from stratified to intermittent flow in small angle upflows. Int. J. Multiphase Flow 27, 599–616.
Soleimani, A., Hanratty, T.J., 2003. Critical liquid flows for the transition from the pseudo-slug and stratified patterns to slug flow. Int. J. Multiphase Flow 29, 51–67.
Taitel, Y., Dukler, A., 1976. A model for predicting flow regime transitions in horizontal and near horizontal gas–liquid flow. AIChE J. 22, 47–55.
Tronconi, E., 1990. Prediction of slug frequency in horizontal two-phase slug flow. AIChE J. 36, 701–709.
Woods, B.D., Hanratty, T.J., 1999. Influence of Froude number on physical processes determining frequency of slugging in horizontal gas–liquid flows. Int. J. Multiphase Flow 25, 1195–1223.
Woods, B.D., Hanratty, T.J., 2000. Mechanism of slug formation in downwardly inclined pipes. Int. J. Multiphase Flow 26, 977–998.
Wu, H.L., Pots, B.F.M., Hollenberg, J.F., Meerhoff, R., 1987. Flow pattern transitions in two-phase gas/condensate flow at high pressure in an 8-inch horizontal pipe. In: Proceedings of BHRA Conference, The Hague, The Netherlands, pp. 13–21.